Tetrahedron 68 (2012) 6284–6288

Contents lists available at SciVerse ScienceDirect

Tetrahedron

journal homepage: www.elsevier.com/locate/tet

Novel piperidine-fused benzoxazino- and quinazolinonaphthoxazines—synthesis and conformational study

Renáta Csütörtöki [a], István Szatmári [a], Matthias Heydenreich [b], Andreas Koch [b], Ines Starke [b], Ferenc Fülöp [a,*], Erich Kleinpeter [b,*]

[a] Institute of Pharmaceutical Chemistry and Stereochemistry Research Group of Hungarian Academy of Sciences, University of Szeged, H-6720 Szeged, Eötvös u. 6, Hungary
[b] Department of Chemistry, University of Potsdam, Karl-Liebknecht-Str. 24-25, D-14476 Potsdam (Golm), Germany

ARTICLE INFO

Article history:
Received 17 April 2012
Accepted 14 May 2012
Available online 22 May 2012

Keywords:
Quinazolines
Naphthoxazines
DFT structural study
Conformational analysis
NMR spectroscopy

ABSTRACT

The reactions of 1-(amino(2-hydroxyphenyl)methyl)-2-naphthol (**3**) and 1-(amino(2-aminophenyl) methyl)-2-naphthol (**6**) with glutardialdehyde resulted in the formation of piperidine-fused benzoxazinonaphthoxazine **4** and quinazolinonaphthoxazine **7**, respectively, both in diastereopure form.
The full conformational search protocols of **4** and **7** were successfully carried out by NMR spectroscopy and accompanying molecular modelling; the global minimum-energy conformers of all diastereomers were computed, and the assignments of the most stable stereoisomers, G^1_{tct} for **4** and G^1_{tct} for **7**, were corroborated by spatial NOE information relating to the H_{7a}-H_{10a}-H_{15b} and H,H coupling patterns of the protons in the flexible part of the piperidine moiety. Additionally, mass spectrometric fragmentation was investigated in collision-induced dissociation experiments. The elemental compositions of the ions were determined by accurate mass measurements.

1. Introduction

The Mannich reaction, between formaldehyde, a secondary amine and a carbon nucleophile, is one of the most important reactions in organic synthesis.[1,2] In a modified Mannich reaction, electron-rich aromatic compounds, such as 1- or 2-naphthol are applied as carbon nucleophiles,[3] e.g., for the successful synthesis of highly functionalized aminonaphthols, such as 1-(amino(2-hydroxyphenyl)methyl)-2-naphthol (**3**)[4] and 1-(amino(2-aminophenyl)methyl)-2-naphthol (**6**).[5]

Aminodiol **3** was earlier transformed to naphth[1,2-*e*][1,3]oxazino[3,4-*c*][1,3]benz-oxazine derivatives by its reaction with formaldehyde and benzaldehyde. The ring-closure reactions proceeded selectively, or in both positions, e.g., the reaction of **3** with 2 equiv of formaldehyde led to the formation of the parent naphth[1,2-*e*][1,3]oxazino[3,4-*c*][1,3]benzoxazine, while for substitution of the ring system at positions 8 and 10, **3** was first treated with 1 equiv of benzaldehyde, followed by the reaction with formaldehyde or phosgene.[4] Additionally, the 8,10-substituted naphth[1,2-*e*][1,3]oxazino[3,4-*c*]quinazoline derivative was isolated from the ring-closure reaction of diamine **6** with formaldehyde, benzaldehyde and/or phosgene.[5]

The highly functionalized aminonaphthols **3** and **6** were further successfully transformed to benzoxazine- or quinazoline-fused naphthoxazines through their reactions with (mainly) mono-oxo reactants. In order to capitalize on all three functional groups in compounds **3** and **6** at the same time, our present aim was to investigate their reactions with dialdehydes, with a view to obtaining new hetero- and polycyclic compounds (Scheme 1). The heterocyclic moiety in **4** and **7** is flexible, and we therefore carried out their detailed conformational analysis by NMR spectroscopy and accompanying molecular modelling. A parallel MS study allowed some stereochemical conclusions.

2. Results and discussion

2.1. Syntheses

The starting aminodiol (**3**) was synthetized by the aminoalkylation of 2-naphthol (**1**) with 2 equiv of salicylaldehyde in the presence of ammonia, followed by acidic hydrolysis of the intermediate napthoxazine (**2**) with TFA.[4]

In order to transform **3** to the desired piperidine-fused benzoxazinonaphthoxazine derivative **4**, aminodiol **3** was dissolved in EtOH and 1.1 equiv of aqueous glutardialdehyde solution was added. The mixture was stirred for 1 day at room temperature, during which white crystals separated out. Preliminary 2D NMR

* Corresponding authors. E-mail addresses: fulop@pharm.u-szeged.hu (F. Fülöp), ekleinp@uni-potsdam.de (E. Kleinpeter).

0040-4020/$ – see front matter © 2012 Elsevier Ltd. All rights reserved.
doi:10.1016/j.tet.2012.05.048

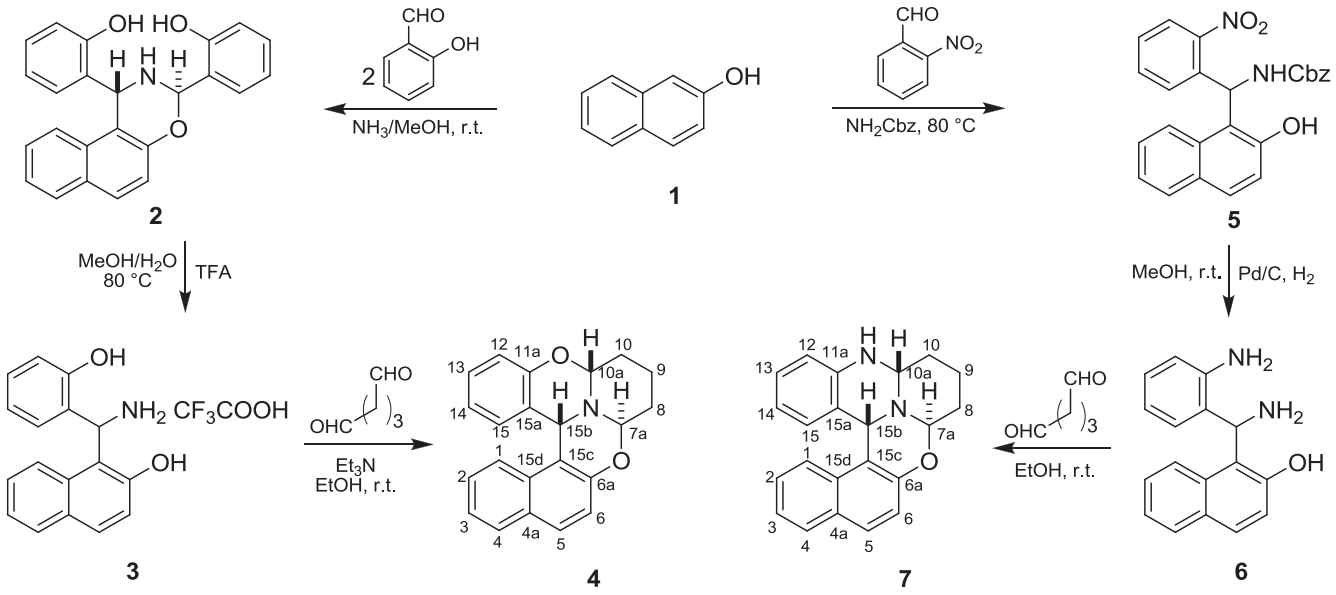

Scheme 1. Syntheses of piperidine-fused naphthoxazine derivatives **4** and **7**.

measurements on the precipitating crystals suggested the expected structure of **4** (Scheme 1).

The synthesis of the analogous piperidine-fused quinazolino-naphthoxazine derivative **7** was planned from 1-(amino(2-aminophenyl)methyl)-2-naphthol (**6**), which was prepared according to the literature procedure.[5] The reaction of **1**, benzyl carbamate and 2-nitrobenzaldehyde resulted in the formation of **5**. This was followed by removal of the protecting group and reduction of the nitro group by catalytic (Pd/C) hydrogenation, yielding **6** (Scheme 1).

A mixture of diamine **6** and 1.1 equiv of aqueous glutardialdehyde solution was dissolved in EtOH and stirred at room temperature. After 3 h, when TLC indicated no more starting material, the reaction mixture was concentrated to dryness and the product was isolated by column chromatography and crystallized from *n*-hexane. The 2D NMR spectra of the isolated compound proved the structure of **7**.

During the ring-closure reactions of **3** and **6** with glutardialdehyde, two new asymmetric centres are introduced, and the formation of four diastereomers is therefore possible; the diastereomeric ratio was checked from the NMR spectra of the crude products. It was found that only a single diastereomer was formed during the reaction. In the NOESY spectra of the purified **4** and **7**, the weak interactions between H_{7a} and H_{15b} and between H_{7a} and H_{10a} proved their trans arrangement, while the presence of a strong cross-peak between H_{10a} and H_{15b} demonstrated their cis arrangement.

In order to extend the series of newly synthetized hexacyclic ring systems, e.g., to the syntheses of pyrrolidine- and azepane-fused naphthoxazine derivatives, our attention focused on the reactions of aminodiol **3** and diamine **6** with succindialdehyde[6] and adipic dialdehyde.[7] However, these reactions did not result in the desired polycyclic compounds either at room temperature or at higher temperature (80–90 °C, classical heating or MW), e.g., at room temperature there was no conversion, while the higher temperature led to decomposition of the starting **3** and **6**.

2.2. Conformational analysis

The conformational search protocol involved PM3 geometry minimization, followed by geometry optimization without restrictions. All calculations were carried out by using the Gaussian 09 program package.[8] Density functional theory calculations were carried out at the B3LYP/6-31G** level of theory.[9a,b] The molecular modelling software package SYBYL 7.3 was used to display results and geometries.[10] As the NMR measurements were recorded in CD_2Cl_2, the energies of the participating conformers were calculated with consideration of the effect of the solvent too (CH_2Cl_2). Compounds **4** and **7** were studied in all the configurations at the DFT level of theory with respect to the preferred conformers and conformational equilibria. Theoretical calculations were performed for all of the stereoisomers of **4** and **7** as regards the *R*/*S* stereochemistry of the involved chiral centres C_{7a}, C_{10a}, C_{15b} and N_{16}. The results of the optimization are given in Table 1 for **4** and in Table 2 for **7**.

It can be concluded from the relative energies of the stereoisomers that the trans arrangement of H_{7a} and H_{15b}, the cis arrangement of H_{10a} and H_{15b} and the trans arrangement of H_{7a} and H_{10a} were preferred for both **4** and **7** (Tables 1 and 2); on the energy hypersurface, the cis/cis/cis and cis/trans/trans isomers display energies of 6.1 kcal/mol and 3.8 kcal/mol, respectively. These computational results were corroborated by the NOE measurements on **4** and **7** (vide supra).

Figs. 1 and 2 depict the three lowest-energy geometries for **4** and **7**, respectively.

Table 1
Calculated energy differences for **4**

Geometries	H_{7a}–H_{15b}	H_{10a}–H_{15b}	H_{7a}–H_{10a}	ΔE (kcal/mol) (in the gas phase)	ΔE (kcal/mol) (in CH_2Cl_2)
G^1_{tct}	trans	cis	trans	0	0
G^2_{ccc}	cis	cis	cis	6.39	6.10
G^3_{ccc}	cis	cis	cis	6.44	5.97
G^4_{ctt}	cis	trans	trans	7.62	7.63
G^5_{ttc}	trans	trans	cis	11.24	11.38
G^6_{ttc}	trans	trans	cis	11.34	10.84
G^7_{ctt}	cis	trans	trans	13.15	12.89
G^8_{tct}	trans	cis	trans	18.33	18.08

The numbers correspond to the following relative configurations: $^1C_{15b}(S^*)$, $N_{16}(R^*)$, $C_{7a}(R^*)$, $C_{10}(R^*)$; $^2C_{15b}(S^*)$, $N_{16}(R^*)$, $C_{7a}(S^*)$, $C_{10}(R^*)$; $^3C_{15b}(S^*)$, $N_{16}(S^*)$, $C_{7a}(S^*)$, $C_{10}(R^*)$; $^4C_{15b}(S^*)$, $N_{16}(R^*)$, $C_{7a}(S^*)$, $C_{10}(S^*)$; $^5C_{15b}(S^*)$, $N_{16}(R^*)$, $C_{7a}(R^*)$, $C_{10}(S^*)$; $^6C_{15b}(S^*)$, $N_{16}(S^*)$, $C_{7a}(R^*)$, $C_{10}(S^*)$; $^7C_{15b}(S^*)$, $N_{16}(S^*)$, $C_{7a}(S^*)$, $C_{10}(S^*)$; $^8C_{15b}(S^*)$, $N_{16}(S^*)$, $C_{7a}(R^*)$, $C_{10}(R^*)$.

Table 2
Calculated energy differences for **7**

Geometries	H_{7a}–H_{15b}	H_{10a}–H_{15b}	H_{7a}–H_{10a}	ΔE (kcal/mol) (in the gas phase)	ΔE (kcal/mol) (in CH_2Cl_2)
G^1_{tct}	trans	cis	trans	0	0
G^2_{ccc}	cis	cis	cis	4.13	3.77
G^3_{ctt}	cis	trans	trans	5.61	5.46
G^4_{ttc}	trans	trans	cis	8.19	7.67
G^4_{ccc}	cis	cis	cis	8.20	7.99
G^5_{ctt}	cis	trans	trans	10.22	9.88
G^6_{ttc}	trans	trans	cis	10.48	10.73
G^7_{tct}	trans	cis	trans	17.61	17.32

The numbers correspond to the following relative configurations: $^1C_{15b}(S^*)$, $N_{16}(R^*)$, $C_{7a}(R^*)$, $C_{10}(S^*)$; $^2C_{15b}(S^*)$, $N_{16}(S^*)$, $C_{7a}(S^*)$, $C_{10}(S^*)$; $^3C_{15b}(S^*)$, $N_{16}(R^*)$, $C_{7a}(S^*)$, $C_{10}(R^*)$; $^4C_{15b}(S^*)$, $N_{16}(S^*)$, $C_{7a}(R^*)$, $C_{10}(R^*)$; $^5C_{15b}(S^*)$, $N_{16}(R^*)$, $C_{7a}(S^*)$, $C_{10}(S^*)$; $^6C_{15b}(S^*)$, $N_{16}(S^*)$, $C_{7a}(S^*)$, $C_{10}(R^*)$; $^7C_{15b}(S^*)$, $N_{16}(R^*)$, $C_{7a}(R^*)$, $C_{10}(R^*)$; $^8C_{15b}(S^*)$, $N_{16}(S^*)$, $C_{7a}(R^*)$, $C_{10}(S^*)$.

No really preferred conformation of the three flexible saturated/partly saturated heterocyclic ring moieties (benzoxazine *bo* and quinazoline *q*, respectively, naphthoxazine *no* and piperidine *p*) was found.

The lowest-energy conformers, G^1_{tct} for **4** and G^1_{tct} for **7**, of the two trans/cis/trans isomers are conformationally identical: *bo*, *q* (*half-chair*), *no* (*twist*) and *p* (*chair*). The chair conformation of the piperidine moiety was proved by proton spectrum iteration[11] of the frozen $-C_{10a}H-C_{10}H_2-C_9H_2-C_8H_2-C_{7a}H-$ unit delivering the expected large coupling constants ^3J(ax,ax) and ^2J(ax,eq) and the much smaller ^3J(ax,eq) and ^3J(eq,eq) (cf. Fig. 3).

As the two G^1_{tct} minimum-energy conformers of **4** and **7** are the experimentally available ones, the congruence of the experimental NMR and the computational study can be concluded. For the same reasons, experimental information concerning the energetically next lowest conformers is not available: G^2_{ccc} of **4** occurs as the *bo* (*twist*), *no* (*boat*), *p* (*twist-boat*) conformer, G^3_{ccc} of **4** as the *bo* (*half-chair*), *no* (*twist-boat*), *p* (*chair*) conformer and the two *N*-analogues G^2_{ccc} of **7** as the *q* (*twist-boat*), *no* (*half-chair*), *p* (*chair*) conformers and G^3_{ctt} of **7** as the *q* (*half-chair*), *no* (*boat*), *p* (*twist-chair*) conformers.

The trans isomer of fused ring perhydrooxazines is usually more stable than the related cis isomer, as reflected in the mass spectra by a larger abundance of the molecular ion of the trans isomer.[12] The mass spectra of similar *O*,*N*-heterocycles were studied previously in detail by means of high-resolution mass spectrometry (MS) and metastable ion analysis.[12–16]

The electron ionization mass spectra of **4** and **7** were investigated and the compositions of the prominent ions were determined via accurate mass measurements. The most important fragment ions and the elemental compositions are listed in the Experimental section. Since it is well known that the appearance potentials of main fragment ions can depend on the stereochemistry of the compounds, low-energy mass spectra (20 eV) of **4** and **7** were first recorded (Table 3).

In order to acquire a deeper insight into the fragmentations of **4** and **7**, we also recorded the mass spectra generated by positive electrospray ionization (ESI). The corresponding ions $[M+H]^+$ and the fragment ions resulting from 'In Source CID' experiments were used as precursor ions and their CID fragmentations were studied. The main results of the ESI-MS/MS measurements are presented in Table 4.

The EI fragmentations differ from the ESI mass spectra in that ions $[M-CHO]^+$, $[M-OH]^+$ and $[M-C_4H_7]^+$ were not found in the ESI-MS/MS mass spectra. The molecular ion peak is the base peak for both compounds. The mass spectra of **4** and **7**, which differ only in the benzoxazine **4** and quinazoline **7** ring moieties, reveal very similar main fragmentation pathways. As expected and characteristic for naphthoxazine moieties, the EI mass spectra of **4** and **7** are dominated by fragmentations such as OH loss and ring-cleavage reactions. OH loss requires hydrogen migration after ionization and ring opening. Compounds **4** and **7** undergo fragmentation mainly involving multiple bond cleavages within the fused ring systems, ionization occurs on the bridgehead *N*-atom.[17] One of the most important fragmentation routes proved to be the loss of C_5H_8N to yield the ion at *m*/*z* 247 for **4** and at *m*/*z* 246 for **7**. The ion

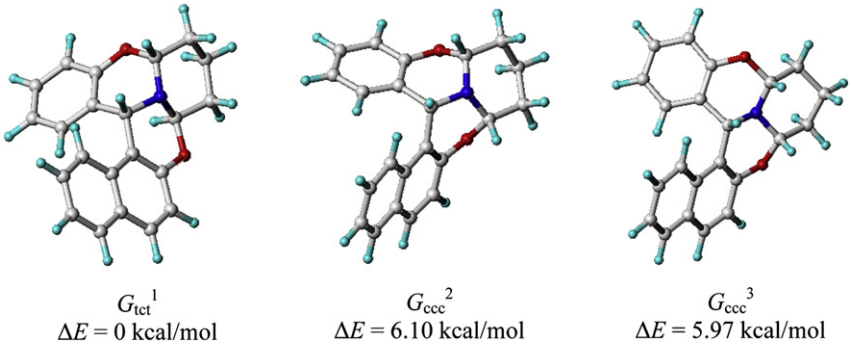

Fig. 1. Minimum-energy conformers of **4**.

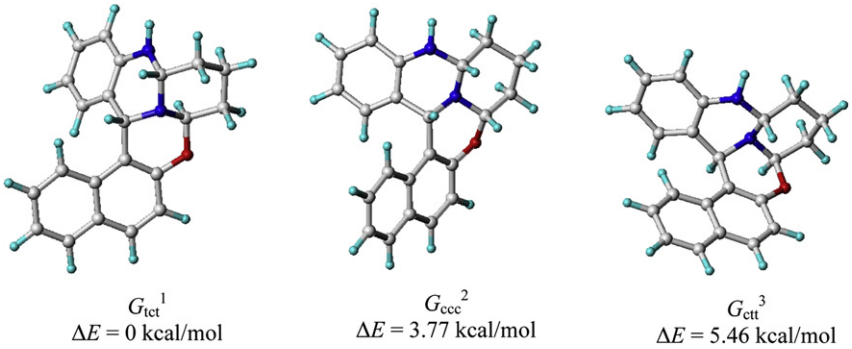

Fig. 2. Minimum-energy conformers of **7**.

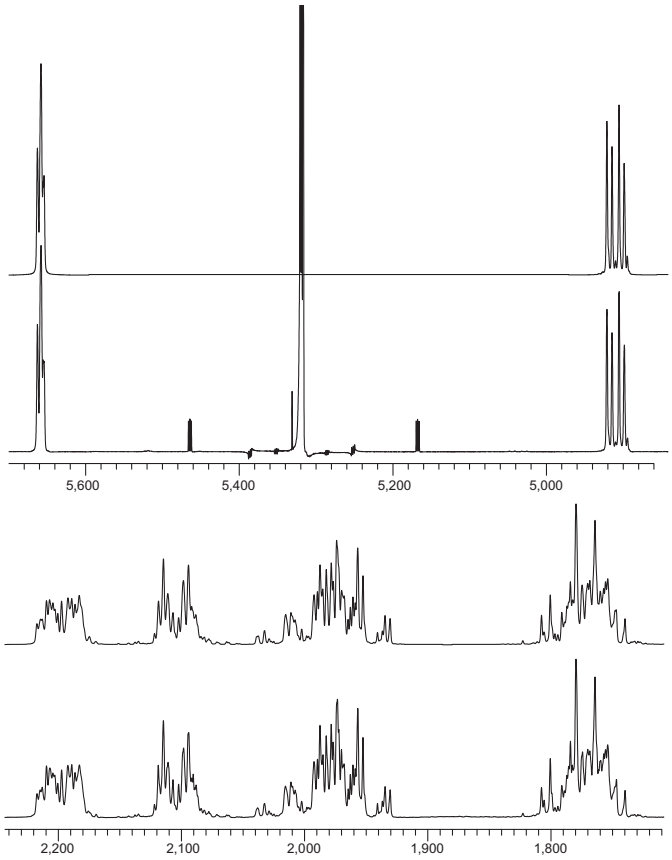

Fig. 3. PERCH iteration of protons H-7a–H-10a of **4** (top: iterated, bottom: observed spectrum); results δ: H-10a (5.66), H-10eq (2.10), H-10ax (1.96), H-9ax (1.99), H-9eq (1.765), H-8eq (2.196), H-8ax (1.77), H-7A (4.91); ^{n}J(H,H): 10a,10eq (2.63), 10a,10ax (2.54), 10a,9ax (0.51), 10a,9eq (0.77), 10eq,10ax (−13.81), 10eq,9ax (3.845), 10eq,9eq (2.61), 10eq,8eq (1.94), H-10eq,H-8ax (−0.25), H-10ax,H-9ax (13.49), H-10ax,H-9eq (4.37), H-10ax,H-8eq (−0.335), H-10ax,H-8ax (−0.39), H-9ax,H-9eq (−13.67), H-9ax,H-8eq (3.63), H-9ax,H-8ax (14.12), H-9ax,H-7a (−0.405), H-9eq,H-8eq (3.06), H-9eq,H-8ax (4.24), H-9eq,H-7a (−0.57), H-8eq,H-8ax (−12.55), H-8eq,H-7a (4.08), H-8ax,H-7a (9.92).

Table 3
EI-MS data from low-energy (20 eV) mass spectra and relative abundances (RAs) [*m*/*z* (%)] corresponding to the main electron-induced fragmentations of **4** and **7**

Ions	Compound **4**	Compound **7**
$[M-C_2H_3O]^+$	286(20)	285(5)
$[M-C_4H_7]^+$	274(6)	273(20)
$[M-C_5H_8N]^+$	247(25)	246(5)
$[M-C_5H_9N_2]^+$	—	231(20)
$[M-C_5H_8NO]^+$	231(100)	—
$C_5H_8N^+$	82(17)	82(3)
$C_4H_7^+$	55(25)	55(8)

$C_{17}H_{11}O^+$ at *m*/*z* 231 is typical for compounds derived from (1-aminobenzyl)-2-naphthol derivatives. A possible mechanism for the multiple bond cleavage, required to form $C_{17}H_{11}O^+$, was described previously for naphthoxazinobenzoxazines.[13] The ESI-MS/MS measurements showed that $C_{17}H_{11}O^+$ at *m*/*z* 231 loses CHO• and forms $C_{16}H_{10}^{+\bullet}$ at *m*/*z* 202.

Table 4
Characteristic fragment ions of **4** and **7** as proved by collision-induced decomposition of the selected precursor ion from ESI positive spectra

Compd	MS from *m*/*z*	Ions
4	$[M+H]^+$ 330	287$[M-C_2H_3O]^+$, 249$[M-C_5H_7N]^+$, 231$[M-C_5H_8NO]$
	231	202$[M-CHO]^+$
7	$[M+H]^+$ 329	312$[M-OH]^+$, 246$[M-C_5H_8N]^+$, 231$[M-C_5H_9N_2]^+$
	231	202$[M-CHO]^+$

The ions at *m*/*z* 231 resulting from the losses of 97 ($C_5H_9N_2$) and 98 (C_5H_8NO) directly from the molecular ions are more abundant in the case of **4** (100%) than for **7** (20%, Table 3). Additionally, the ions $C_4H_7^+$ at *m*/*z* 55 and $C_5H_8N^+$ at *m*/*z* 82 are more abundant for **4**, while the ion at *m*/*z* 247 resulting from loss of the piperidine ring is more abundant for **4** (25%) than for **7** (*m*/*z* 246, RA 5%). The type of heteroatom (O for **4**, NH for **7**) at position 11 also has an effect on the loss of C_2H_3O• to yield the ion at *m*/*z* 286 for **4** and *m*/*z* 285 for **7**.

Previous NMR investigations on naphth[1,2-*e*][1,3]oxazino[3,4-*c*][1,3]benzoxazine revealed the trans orientation of the C_{15a}–C_{15b} bond to the lone pair of N_9, while the preferred conformation of the benzoxazine and naphthoxazine rings was found to be a *twisted chair*.[4] The intensities of the fragment ions at *m*/*z* 231 (100%) and *m*/*z* 247 (22%) in the mass spectra of **4** can be compared with those of the corresponding ions, in the mass spectra of naphth[1,2-*e*][1,3]oxazino[3,4-*c*][1,3]benzoxazine.[13] Similar intensities of the typical fragment ions, together with the NMR results (vide supra), corroborate the conformations of the two heterocyclic ring systems in **4**—the *twisted chair* and the G^1_{tct} configuration as obtained from DFT calculations and depicted in Fig. 2.

In the low-energy mass spectra, the higher RA of the fragment ions at *m*/*z* 286 in **4** (20%) than in **7** (*m*/*z* 285 only 5%) proves that the elimination of C_2H_3O from **4** is more favourable because of the higher ring strain in **4**. The higher RAs of the fragment ions *m*/*z*: 231, 247 and 286 can be explained by the stronger electronic and steric effects in **4** with the benzoxazine moiety.

3. Conclusions

Piperidine-fused benzoxazinonaphthoxazine **4** was synthetized through the reaction of 1-(amino(2-hydroxyphenyl)methyl)-2-naphthol (**3**) with glutardialdehyde, while piperidine-fused quinazolinonaphthoxazine **7** was prepared analogously from 1-(amino(2-aminophenyl)methyl)-2-naphthol (**6**). The most stable stereoisomers, G^1_{tct} for **4** and G^1_{tct} for **7**, were identified by theoretical calculations at the DFT level of theory, considering the solvent, corroborated by spatial NOE information between $H_{7a}/H_{10a}/H_{15b}$ and ^{1}H NMR spectrum iteration: the H,H coupling patterns of the protons in the flexible part of the piperidine ring moiety proved the frozen chair conformation.

4. Experimental section

4.1. General

Melting points were determined on a Hinotek X-4 type melting point apparatus and are uncorrected.

The different conformations and configurations of the studied compounds were preoptimized with the PM3 Hamiltonian.[18] The B3LYP density functional method was selected for all calculations. The method was based on Becke's three-parameter hybrid functionals[19] and the correlation functional of Lee et al.[20] All optimizations were carried out without any restriction at the B3LYP/6-31G** level of theory.[9a,b] The self-consistent reaction field method and the integral equation formalism variant of the polarizable continuum model were applied to take solvent effects (CD_2Cl_2) into account.[21] Visualization was carried out with the modelling software SYBYL 7.3.[10]

The ^{1}H and ^{13}C NMR spectra were recorded on CD_2Cl_2 solutions in 5 mm tubes, at room temperature, on a Bruker Avance III spectrometer, at 600.13 (^{1}H) and 150.61 (^{13}C) MHz, with the deuterium signal of the solvent as the lock and TMS as internal standard. All spectra (^{1}H, ^{13}C, gs-H,H-COSY, gs-HMQC, gs-HMBC and NOESY) were acquired and processed with the standard Bruker software. The low-resolution EI mass spectra of **4** and **7** were obtained by

using a GC–MS TRACE DSQ II mass spectrometer (Thermo Fisher Scientific Dreieich, Germany), with an electron energy of 70 eV and a source temperature of 180 °C, using a direct insertion probe with a direct desorption probe filament in positive ion mode. The HRMS EI spectra were recorded at 70 eV and 20 eV, using a GC/MS instrument with a time-of-flight mass analyser (Micromass, Waters, Manchester, UK) in positive ion mode. Below 20 eV, the production of ions was not sufficient. The elemental compositions of the ions were determined by accurate mass measurements with standard deviation <5 ppm. Perfluorokerosene was used as reference compound and the mass resolution was 5000.

The ESI spectra were recorded with a UHR-Q-TOF maXis (Bruker Daltonik GmbH, Bremen, Germany) mass spectrometer in positive electrospray mode. All samples were injected (3 μL/min) with a Harvard syringe pump. The capillary voltage was set to 4.0 kV.

The desolvation temperature was 180 °C. The desolvation gases were delivered at 4.0 L/min. For MS/MS after selection of the appropriate precursor ion, nitrogen was used as collision gas and the gas cell was maintained between 5 and 65 eV.

Starting trifunctional aminonaphthols were synthetized according to literature methods: **3**[4] and **6**.[5]

4.2. Synthesis of 4

Et_3N (0.15 mL, 1.1 mmol) and aqueous glutardialdehyde solution (25%, 0.42 mL, 1.1 mmol) were added to a solution of **3** (379 mg, 1 mmol) in EtOH (15 mL). The mixture was stirred for 1 day at room temperature, during which white crystals separated out. The crystalline product (**4**) was filtered off, washed with cold EtOH (2×5 mL) and recrystallized from iPr_2O (10 mL).

White crystals, 267 mg (81%), mp: 207–209 °C. ^{1}H NMR (600 MHz, CD_2Cl_2): δ=1.73–1.81 (m, 2H, 9-H_{eq}, 8-H_{ax}), 1.92–2.02 (m, 2H, 10-H_{ax}, 9-H_{ax}), 2.08–2.12 (m, 1H, 10-H_{eq}), 2.17–2.22 (m, 1H, 8-H_{eq}), 4.91 (dd, 1H, J=9.4, 5.4 Hz, 7a-H), 5.64–5.66 (m, 1H, 10a-H), 5.88 (s, 1H, 15b-H), 6.62 (td, 1H, J=7.5, 1.1 Hz, 14-H), 6.78–6.82 (m, 2H, 15-H, 12-H), 7.05 (d, 1H, J=8.9 Hz, 6-H), 7.11 (t, 1H, J=7.7 Hz, 13-H), 7.39 (td, 1H, J=7.6, 0.9 Hz, 3-H), 7.52 (td, 1H, J=7.4, 1.4 Hz, 2-H), 7.74 (d, 1H, J=8.9 Hz, 5-H), 7.81–7.85 (t, 2H, J=8.1 Hz, 4-H, 1-H). ^{13}C NMR (150 MHz, CD_2Cl_2): δ=16.9 (C-9), 30.4 (C-10), 31.2 (C-8), 53.8 (C-15b), 81.1 (C-7a), 87.3 (C-10a), 114.1 (C-15c), 116.4 (C-12), 118.8 (C-6), 120.3 (C-14), 122.0 (C-15a), 123.1 (C-1), 123.8 (C-3), 127.3 (C-2), 128.9 (C-4), 129.0 (C-4a), 129.1 (C-13, C-15), 129.8 (C-5), 132.9 (C-15d), 150.4 (C-6a), 153.1 (C-11a).

HR-EI-MS formula and RA (%): $[M]^{+\cdot}$ (100) m/z calcd for $C_{22}H_{20}NO_2$: 329.1410, found 329.1427; $[M-OH]^+$ (92) m/z calcd for $C_{22}H_{18}NO$: 312.1388; found 312.1377; $[M-CHO]^+$ (5) m/z calcd for $C_{21}H_{18}NO$: 300.1383, found 300.1378; $[M-C_2H_3O]^+$ (6) m/z calcd for $C_{20}H_{16}NO$: 286.1232, found 286.1238; $[M-C_5H_8N]^+$ 247(20); m/z calcd for $C_{17}H_{11}O_2$: 247.0754, found 247.0758; $[M-C_5H_8NO]^+$ (100) m/z calcd for $C_{17}H_{11}O$: 231.0804, found 231.0807; $[M-H]^+$ 328(25), $C_{16}H_{10}O^{+\bullet}$: 218(10), $C_{16}H_{10}^{+\bullet}$: 202(10), $C_{15}H_9^+$: 189(24).

4.3. Synthesis of 7

To a solution of **6** (264 mg, 1 mmol) in EtOH (15 mL), aqueous glutardialdehyde solution (25%, 0.42 mL, 1.1 mmol) was added and the mixture was stirred at room temperature. After 3 h, when TLC indicated no presence of the starting materials, the reaction mixture was concentrated under reduced pressure. The product was then isolated by column chromatography (eluent: *n*-hexane/EtOAc 2:1 v/v) and was crystallized from *n*-hexane.

Beige crystals, 141 mg (43%), mp: 197–199 °C. ^{1}H NMR (600 MHz, CD_2Cl_2): δ=1.69–1.71 (m, 1H, 9-H_{eq}), 1.72–1.74 (m, 1H, 8-H_{ax}), 1.74–1.79 (m, 1H, 10-H_{ax}), 1.94–1.98 (m, 1H, 9-H_{ax}), 1.99–2.04 (m, 1H, 10-H_{eq}), 2.14–2.19 (m, 1H, 8-H_{eq}), 3.99 (br s, 1H, NH), 4.85 (dd, 1H, J=9.4, 4.1 Hz, 7a-H), 5.17–5.19 (m, 1H, 10a-H), 5.78 (s, 1H, 15b-H), 6.37 (td, 1H, J=7.5, 1.1 Hz, 14-H), 6.51 (dd, 1H, J=8.0, 1.1 Hz, 12-H), 6.59 (d, 1H, J=7.7 Hz, 15-H), 6.97 (t, 1H, J=7.6 Hz, 13-H), 7.04 (d, 1H, J=8.9 Hz, 6-H), 7.36 (ddd, 1H, J=8.1, 6.9, 1.1 Hz, 3-H), 7.49 (ddd, 1H, J=8.4, 6.9, 1.4 Hz, 2-H), 7.73 (d, 1H, J=8.9 Hz, 5-H), 7.80 (d, 1H, J=8.3 Hz, 1-H), 7.81 (d, 1H, J=8.1 Hz, 4-H). ^{13}C NMR (150 MHz, CD_2Cl_2): δ=16.8 (C-9), 30.7 (C-10), 31.6 (C-8), 55.2 (C-15b), 67.3 (C-10a), 81.5 (C-7a), 113.6 (C-12), 114.9 (C-15c), 117.2 (C-14), 118.7 (C-6), 119.6 (C-15a), 123.0 (C-1), 123.4 (C-3), 127.0 (C-2), 128.3 (C-13), 128.7 (C-4), 128.8 (C-4a), 129.2 (C-15), 129.3 (C-5), 132.9 (C-15d), 142.1 (C-11a), 150.3 (C-6a).

HR-EI-MS formula and RA (%): $[M]^{+\cdot}$ (100) m/z calcd for $C_{22}H_{20}N_2O$: 328.1570, found 328.1579; $[M-OH]^+$ (70) m/z calcd for $C_{22}H_{19}N_2$: 311.1543, found 311.1539; $[M-CHO]^+$ (8) m/z calcd for $C_{21}H_{19}N_2$: 299.1543, found 299.1540; $[M-C_2H_3O]^+$ (4) m/z calcd for $C_{20}H_{17}N_2$: 285.1392, found 285.1392; $[M-C_4H_7]^+$ (20) m/z calcd for $C_{18}H_{13}N_2O$: 273.1022, found 273.1026; $[M-C_5H_8N]^+$ 246(14) m/z calcd for $C_{17}H_{12}NO$: 246.0913, found 246.0922; $[M-C_5H_9N_2]^+$ (20) m/z calcd for $C_{17}H_{11}O$: 231.0804; found 231.0807; $[M-H]^+$ 327(20), $C_{16}H_{11}N^{+\bullet}$: 217(10), $C_{16}H_{10}^{+\bullet}$: 202(7), $C_{15}H_9^+$: 189(5).

Acknowledgements

The authors thank the Hungarian Research Foundation (OTKA No. K-75433) and TÁMOP-4.2.1/B-09/KONV-2010-0005 and the Deutsche Akademische Austauschdienst (DAAD), project-ID 50368559, for financial support. I.S. acknowledges the award of a Bolyai János Fellowship.

References and notes

1. Arrayas, R. G.; Carratero, J. C. *Chem. Soc. Rev.* **2009**, *38*, 1940–1948.
2. Martin, S. F. *Pure Appl. Chem.* **2009**, *81*, 195–204.
3. Szatmári, I.; Fülöp, F. *Curr. Org. Synth.* **2004**, *1*, 155–165.
4. Heydenreich, M.; Koch, A.; Klod, S.; Szatmári, I.; Fülöp, F.; Kleinpeter, E. *Tetrahedron* **2006**, *62*, 11081–11089.
5. Csütörtöki, R.; Szatmári, I.; Koch, A.; Heydenreich, M.; Kleinpeter, E.; Fülöp, F. *Tetrahedron* **2011**, *67*, 8564–8571.
6. Kuznetsov, V. F. U.S. Patent 7,855,296, 2010.
7. López, S.; Fernández-Trillo, F.; Midón, P.; Castedo, L.; Saá, C. *J. Org. Chem.* **2005**, *70*, 6346–6352.
8. Frisch, M. J.; Trucks, G. W.; Schlegel, H. B.; Scuseria, G. E.; Robb, M. A.; Cheeseman, J. R.; Scalmani, G.; Barone, V.; Mennucci, B.; Petersson, G. A.; Nakatsuji, H.; Caricato, M.; Li, X.; Hratchian, H. P.; Izmaylov, A. F.; Bloino, J.; Zheng, G.; Sonnenberg, J. L.; Hada, M.; Ehara, M.; Toyota, K.; Fukuda, R.; Hasegawa, J.; Ishida, M.; Nakajima, T.; Honda, Y.; Kitao, O.; Nakai, H.; Vreven, T.; Montgomery, T. A.; Peralta, J. E., Jr.; Ogliaro, F.; Bearpark, M.; Heyd, J. J.; Brothers, E.; Kudin, K. N.; Staroverov, V. N.; Kobayashi, R.; Normand, J.; Raghavachari, K.; Rendell, A.; Burant, J. C.; Iyengar, S. S.; Tomasi, J.; Cossi, M.; Rega, N.; Millam, J. M.; Klene, M.; Knox, J. E.; Cross, J. B.; Bakken, V.; Adamo, C.; Jaramillo, J.; Gomperts, R.; Stratmann, R. E.; Yazyev, O.; Austin, A. J.; Cammi, R.; Pomelli, C.; Ochterski, J. W.; Martin, R. L.; Morokuma, K.; Zakrzewski, V. G.; Voth, G. A.; Salvador, P.; Dannenberg, J. J.; Dapprich, S.; Daniels, A. D.; Farkas, O.; Foresman, J. B.; Ortiz, J. V.; Cioslowski, J.; Fox, D. J. *Gaussian 09, Revision A.02*; Gaussian,: Wallingford CT, 2009.
9. (a) Hehre, W. J.; Radom, L.; v. Rague Schleyer, P.; Pople, J. *Ab Initio Molecular Orbital Theory*; Wiley: New York, NY, 1986; (b) Becke, A. D. *J. Chem. Phys.* **1993**, *98*, 1372–1377.
10. SYBYL 7.3; Tripos: 1699 South Hanley Road, St. Louis, MO 63144, USA, 2007.
11. PERCH Solutions Ltd. Kuopio, Finland Laatikainen, R. *J. Magn. Reson.* **1991**, *92*, 1–9; Laatikainen, R. QCMP100. MLDC8 *QCPE Bull.* **1992**, *12*, 23; Laatikainen, R.; Niemitz, M.; Weber, U.; Sundelin, J.; Hassinen, T.; Vepsäläinen, J. *J. Magn. Reson.* **1996**, *A120*, 1–10; Laatikainen, R.; Niemitz, M.; Malaisse, W. J.; Biesemans, M.; Willem, R. *Magn. Reson. Med.* **1996**, *36*, 359–365.
12. Pihlaja, K.; Liukko-Sipi, S.; Fülöp, F.; Bernáth, G.; Vainiotalo, P. *Rapid Commun. Mass Spectrom.* **1991**, *5*, 230–233.
13. Martiskainen, O.; Fülöp, F.; Szatmári, I.; Pihlaja, F. *Arkivoc* **2009**, *iii*, 115–129.
14. Joutsiniemi, K.; Vainiotalo, P.; Pihlaja, K.; Lázár, L.; Fülöp, F.; Bernáth, G. *Rapid Commun. Mass Spectrom.* **1995**, *9*, 1035–1037.
15. Joutsiniemi, K.; Vainiotalo, P.; Lázár, L.; Fülöp, F.; Bernáth, G. *Rapid Commun. Mass Spectrom.* **1995**, *9*, 998–1002.
16. Vainiotalo, P.; Fülöp, F.; Stájer, G.; Bernáth, G.; Pihlaja, K. *Acta Chem. Scand.* **1990**, *44*, 165–169.
17. Juhász, M.; Zalán, Z.; Fülöp, F.; Pihlaja, K. *Rapid Commun. Mass Spectrom.* **2006**, *20*, 3595–3604.
18. (a) Stewart, J. J. P. *J. Comput. Chem.* **1989**, *10*, 209–220; (b) Stewart, J. J. P. *J. Comput. Chem.* **1989**, *10*, 221–264.
19. Becke, A. D. *J. Chem. Phys.* **1993**, *98*, 5648–5652.
20. Lee, C.; Yang, W.; Parr, R. G. *Phys. Rev. B* **1988**, *37*, 785–789.
21. Tomasi, J.; Mennucci, B.; Cammi, R. *Chem. Rev.* **2005**, *105*, 2999–3093.